Draft version April 29, 2024
Typeset using LaTeX **preprint2** style in AASTeX631

Confirming the g(gravity)-mode Amplitude Pulsations of GD 358*

Jacob Ross Romeo[1] and Laina Tallman Bogusta[1]

[1]*Embry Riddle Aeronautical University*
College of Arts and Science

ABSTRACT

We used the 1-meter observatory at Embry Riddle Aeronautical University (ERAU). Observing with the Photometric CCD, using the G-filter with 60 s exposures. Calibrating the images with AstroImageJ [AIJ (1997)] and performing Fourier analysis with Period04 [P04 (1986)]. This project focuses on confirming the amplitude pulsations and pulsation period of GD 358, a confirmed variable white dwarf (WD) with a helium atmosphere (spectral type DBV). It is located within the narrow instability strip on the WD cooling sequence where ZZ Ceti stars reside. GD 358 exhibits amplitude variations ranging up to 0.3 mag, with a pulsation period between its pulse maximum of 600 s to 700 s. Previous data confirms at least 28 pulsation modes, each with periods ranging from 142.3 s to 952 s [Winget et al. (1982)]. Our observation detected 5 of these frequencies, above the noise level, consistent with previous findings [Winget et al. (1982)]. We identified the principle frequency at 1.419 mHz, with a corresponding period of 705 s and amplitude of 38.4 mmag. This finding aligns with data from two separate papers. Additionally, four other frequencies detected align with the first dataset [Winget et al. (1982)], while three of these also align with the second [Córsico et al. (2022)]. Though three of the five pulsation amplitudes do not align with the second paper, all of the amplitudes align with the first paper. Notably, two of the frequencies we detected were combinatory frequencies as described in the second paper, although our research was not primarily focused on detecting these.

Keywords: Variable White Dwarf – g mode Pulsations – Pulsation Frequency – Differential Photometry – Fourier Analysis – Time Series – Amplitude Spectrum

1. INTRODUCTION

WDs represent the endpoint of stellar evolution for the majority of stars in the universe. GD 358 stands out as a notable example of a variable WD exhibiting g-mode, non-radial pulsations due to it being the first observed DBV pulsator. From the research paper Photometric Observations of GD 358, "Many of the pulsations fall into groups of 4 or 5 modes that are equally spaced in frequency, suggesting that the pulsations are l = 2 g-modes that have been split by rotation". Understanding the pulsation properties of WDs such as GD 358 provides valuable insights into cosmological constants and the internal structure and evolu-

* Released on April, 24th, 2024

tion of these stellar remnants. Such examples are that they are candidates for dark matter, they are microlensing objects and progenitors for type 1a supernovae, and are used as accurate clocks [Winget & Kepler (2008)]. Making the study of variable WDs extremely valuable and essential for further study of the properties of this universe.

In this study, we focus on investigating the amplitude pulsations and pulsation period of GD 358, which is located within the narrow instability strip on the WD cooling sequence. Previous observations have revealed GD 358's amplitude variations, with the principle pulsation period ranging from 600 s to 700 s. Extensive data analysis has identified numerous pulsation modes, each with periods spanning from 142.3 s to 952 s [Winget et al. (1982)] and from 422 s to 1087 s [Córsico et al. (2022)], taken from another study. However, we wanted to further investigate to confirm and characterize these pulsation properties comprehensively.

To photometrically observe this star, we utilized the 1-meter observatory at ERAU, employing the CCD with 60-second exposures in the G-filter for observational data collection. AstroImageJ [AIJ (1997)] was used for data calibration along with differential photometry for making a time series. This was followed by inputting the time series for Fourier analysis into Period04 [P04 (1986)] to extract the amplitude spectrum. Further explanation of the operations and data collection is described in the 2nd section.

Our study aims to validate previous findings regarding GD 358's pulsation behavior and provide new insights into its pulsation characteristics. Though the conditions for observation were poor and the data we received was not as extensive as previous research. Through rigorous data analysis and comparison with existing literature, we hope to add to the growing body of knowledge surrounding GD 358. Inevitably contributing to the understanding of variable WDs and their pulsating behavior as a whole.

2. OBSERVATIONAL DETAILS & METHODS

The ERAU 1-meter telescope is a Ritchey-Chretien reflector using a 100 cm primary mirror with a f/8 focal ratio. Implementing the SBIG imaging CCD with a FOV of 4096x4096x15.8um for photometry [1-M (2024)]. We used this CCD for our observations, imaging GD 358 using the G-filter for 60 s each exposure, which gave sufficient counts for data analysis. We used the G-filter since the star peaks in this filter, where the 60 s exposure was determined through trial and error. Previously we tried calculating the exposure time using the SNR, but the time derived was too short of a window to collect sufficient data. Due to weather, mainly the humidity, we were only able to gather a single night worth of data on March 4, 2024. The night which the data was taken had perfect conditions, showing the airmass plot in Figure 1. Compiling 150 images over a time period of $\approx$ 3 hours and only using 140 out of the 150 images to perform data analysis due to impurities.

Once the images were compiled, we used AstroImageJ [AIJ (1997)] to calibrate the images which included applying dark subtraction, bias subtraction, and flat division. Once this was done, differential photometry was performed to gather the relative flux to make a time series of the database, plotted in Python, shown in Figure 2. The time series was then imported into Period04 [P04 (1986)] to resolve the pulsation frequencies using Fourier analysis. These were then plotted in Python to show the principle frequency and where the noise level resided (Figure 3). We then exported the frequencies found and their respective amplitudes and analytical uncertainties. With these, we were able to compare similarities with known data from the accepted papers studying GD 358.

3. CALCULATIONS

There was little to no math involved in this research due it being primarily conducted through AstroImageJ [AIJ (1997)] and Period04 [P04 (1986)] which did most of the calculations. Figure 2 shows the time series that was plotted from the data collected through AstroImageJ. By adding each amplitude peak, approximately 15, and converting the total time of observation minus the readout time, which was 2.3 hours to be exact, into seconds. The periodicity of GD 358 can be derived by the following, $T = \frac{(2.8hrs)3600s/hrs}{15} = 672s$, which fits the threshold of 600 s to 700s [Winget et al. (1982)].

4. RESULTS

The results found in this research were conclusive with pulsation period and amplitudes found in external papers. The paper by Winget et al. (1982) titled "PHOTOMETRIC OBSERVATIONS OF GD 358," had concluded a frequency of 1.428 mHz based on their data where Córsico et al. (2022) received a frequency of 1.421 mHz. Figure 4 shows a comparison of the amplitude spectrum from Winget et al. (a) and Corsico et al (b). With the amplitude spectrum we derived using P04 (1986) shown in the table below.

Fourier Results of GD 358			
Nr	**Frequency (mHz)**	**Period (s)**	**Amplitude (mmag)**
F1	1.418 ± 0.002	704.8	38.38 ± 1.548
F2	2.656 ± 0.008	376.5	9.71 ± 1.548
F3	1.334 ± 0.009	749.6	9.5 ± 1.548
F4	4.087 ± 0.012	244.7	7.03 ± 1.548
F5	2.845 ± 0.013	351.5	6.21 ± 1.548

Table 1: Data taken by Fourier analysis in Period04 [P04 (1986)] so we are able to compare results with prior research.

APPENDIX

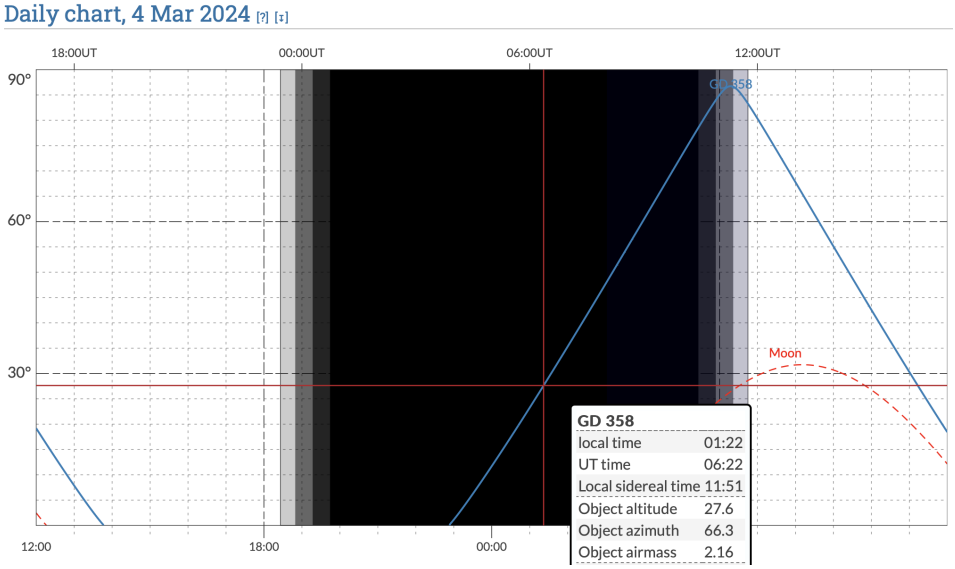

Figure 1. Airmass plot obtained from https://airmass.org showing when GD 358 rises and falls and providing the moon's position throughout the observation period.

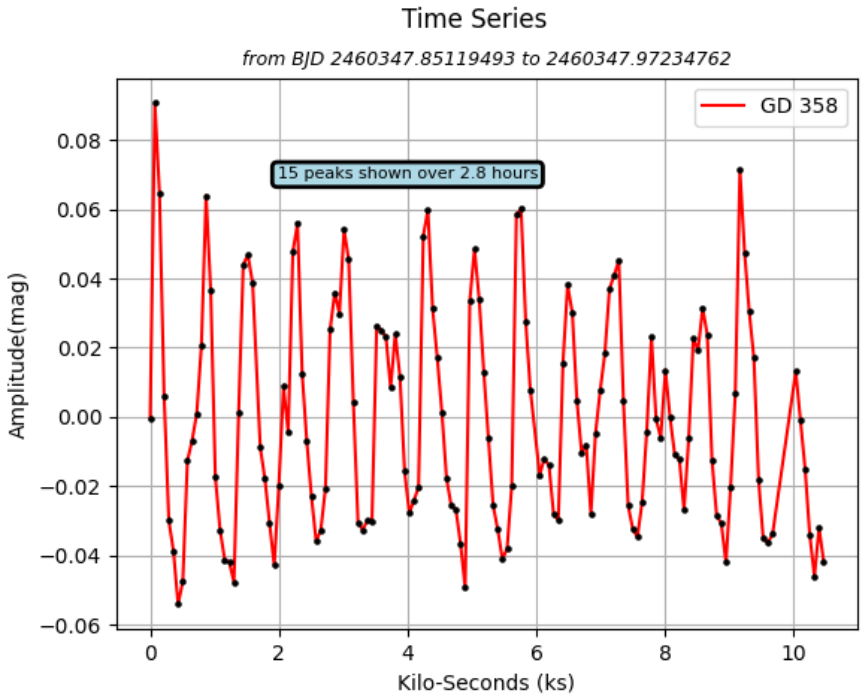

Figure 2. The Time Series of GD 358 made in Python with data analyzed in AstroImageJ where 15 different peaks were observed over a time period of 2.8 hours.

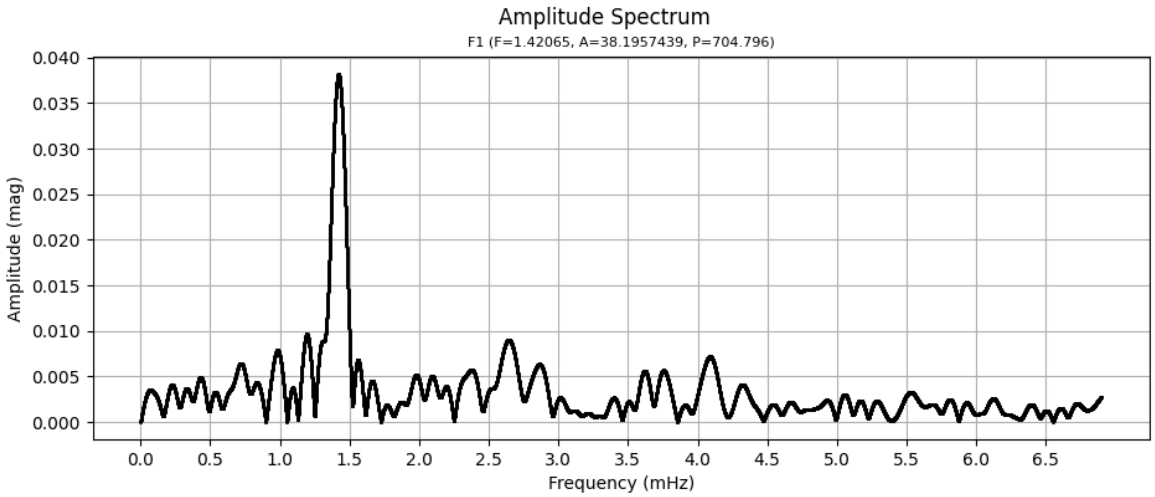

Figure 3. The Amplitude Spectrum made in Python from the Fourier Analysis in Period 04 where you can distinctively see the principle frequency spike.

a)

		Frequency[a] (10^{-3} Hz)	Period (s)	Mean Fractional Semi-Amplitude ($\times 10^{-3}$)
		1.050	952	12.1
	F3	1.246	803	21.2
1	F1	1.428	700	36.1
		1.619	618	38.8
		1.797	557	9.0
		2.367	422	11.5
		2.525	396	7.3
	F2	2.670	375	11.2
2	F5	2.861	349	10.2
		3.047	328	14.5
		3.230	310	11.9
		3.789	263.9	5.2
		3.973	251.7	5.8
	F4	4.105	243.6	5.8
		4.287	233.3	4.6
3		4.473	223.6	3.8
		4.660	214.6	6.5
		4.855	206.0	4.0
		5.057	197.8	2.3
		5.225	191.4	3.5
4		5.406	185.0	3.3
		5.572	179.5	2.8
		5.768	173.4	2.2
		6.289	159.0	3.0
		6.494	154.0	2.3
		6.613	151.2	1.9
		6.756	148.0	1.5
		7.027	142.3	2.2

b)

	Peak	ν (μHz)	Π (s)	A (ppt)
	f_1	919.507 ± 0.018	1087.538 ± 0.021	2.521 ± 0.18
	f_2	1038.177 ± 0.026	963.226 ± 0.025	1.739 ± 0.18
	f_3	1082.770 ± 0.008	923.556 ± 0.007	5.723 ± 0.18
	f_4	1170.146 ± 0.015	854.593 ± 0.011	3.115 ± 0.18
	f_5	1232.928 ± 0.004	811.076 ± 0.003	10.325 ± 0.18
	f_6	1289.082 ± 0.006	775.745 ± 0.003	7.212 ± 0.18
F3	**f_7**	1297.338 ± 0.008	770.808 ± 0.005	5.574 ± 0.18
F1	**f_8**	1421.059 ± 0.004	703.700 ± 0.002	11.782 ± 0.18
	f_9	1435.142 ± 0.018	696.794 ± 0.009	2.530 ± 0.18
	f_{10}	1611.949 ± 0.010	620.367 ± 0.004	4.327 ± 0.18
	f_{11}	1617.409 ± 0.034	618.272 ± 0.013	1.352 ± 0.18
	f_{12}	1623.248 ± 0.013	616.048 ± 0.005	3.403 ± 0.18
	f_{13}	2024.182 ± 0.020	494.026 ± 0.005	2.280 ± 0.18
	f_{14}	2154.064 ± 0.010	464.238 ± 0.002	4.360 ± 0.18
	f_{15}	2157.584 ± 0.042	463.481 ± 0.009	1.109 ± 0.18
	f_{16}	2359.010 ± 0.021	423.906 ± 0.003	2.214 ± 0.18
	f_{17}	2362.689 ± 0.021	423.246 ± 0.003	2.169 ± 0.18
	f_{18}	2366.318 ± 0.019	422.597 ± 0.003	2.380 ± 0.18
	$2f_1$	1839.301 ± 0.031	543.684 ± 0.009	1.498 ± 0.18
	f_3+f_5	2315.669 ± 0.036	431.840 ± 0.006	1.282 ± 0.18
	$2f_5$	2465.756 ± 0.026	405.555 ± 0.004	1.772 ± 0.18
	f_5+f_7	2530.302 ± 0.034	395.209 ± 0.005	1.337 ± 0.18
F2	f_5+f_8	2653.958 ± 0.028	376.795 ± 0.004	1.614 ± 0.18
F5	f_6+f_{12}	2912.290 ± 0.040	343.372 ± 0.004	1.147 ± 0.18
	f_8+f_{12}	3044.295 ± 0.029	328.483 ± 0.003	1.586 ± 0.18
	f_5+f_{14}	3386.984 ± 0.038	295.247 ± 0.003	1.213 ± 0.18

Figure 4. Table of the results that agree with our results in Table 1 [4] from Winget et al. (1982) shown in a) and from Córsico et al. (2022) shown in b).

REFERENCES

1986, Period04. http://period04.net/

1997, AstroImageJ (AIJ). https://www.astro.louisville.edu/software/astroimagej/

2024, Wikimedia Foundation. https://en.wikipedia.org/wiki/Embry-Riddle_Observatory

Córsico, A. H., Uzundag, M., Kepler, S. O., et al. 2022, Astronomy amp; Astrophysics, 659, doi: 10.1051/0004-6361/202142153

Winget, D., & Kepler, S. 2008, Annual Review of Astronomy and Astrophysics, 46, 157–199, doi: 10.1146/annurev.astro.46.060407.145250

Winget, D. E., Robinson, E. L., Nather, R. D., & Fontaine, G. 1982, The Astrophysical Journal, 262, doi: 10.1086/183902